Electronic Supporting Information (ESI)

p−*d* Orbital hybrid Ni-Al NC catalyst withstand potential variations in highly selective electro-reduction of CO_2 to CO

Linjie Wang,[a] Da Zhang,[a] Shaojuan Luo,*[a,c] Yong Xu,[b] and Chuande Wu*[d]

[a]School of Chemical Engineering and Light Industry, Guangdong University of Technology, Guangzhou 510006, China.

[b]Guangzhou Key Laboratory of Low-Dimensional Materials and Energy Storage Devices, Collaborative Innovation Center of Advanced Energy Materials, School of Materials and Energy, Guangdong University of Technology, Guangzhou 510006, China.

[c]Jieyang Branch of Chemistry and Chemical Engineering Guangdong Laboratory, Rongjiang Laboratory, Jieyang, 515200, China.

[d]Department of Chemistry, Zhejiang University, Hangzhou 310000, China.

*Corresponding author kesjluo@gdut.edu.cn

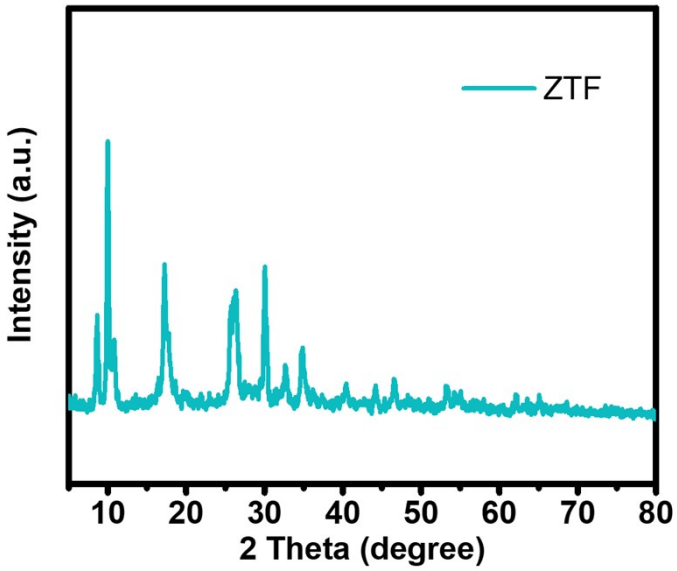

Figure S1. XRD pattern of ZTF.

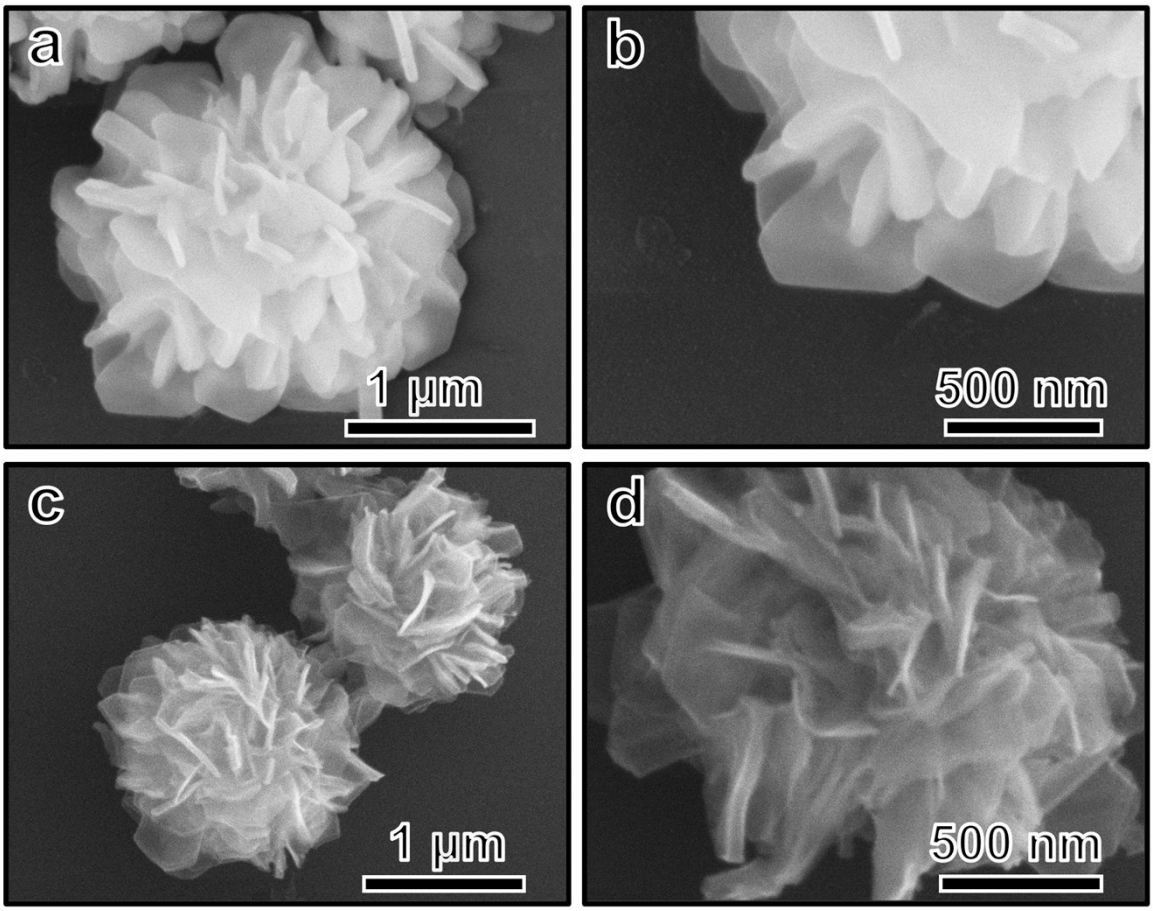

Figure S2. SEM images of (a-b) ZTF and (c-d) NC.

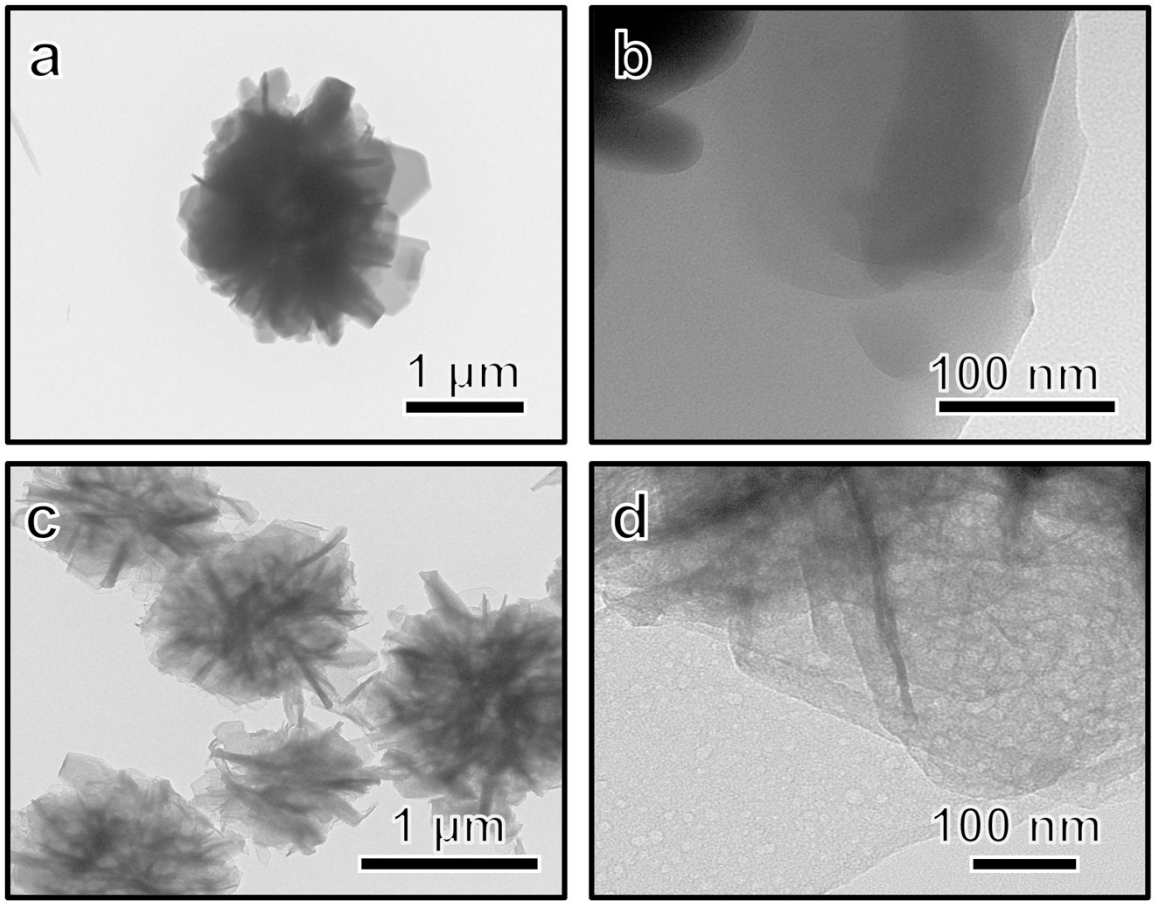

Figure S3. TEM images of (a-b) ZTF and (c-d) NC.

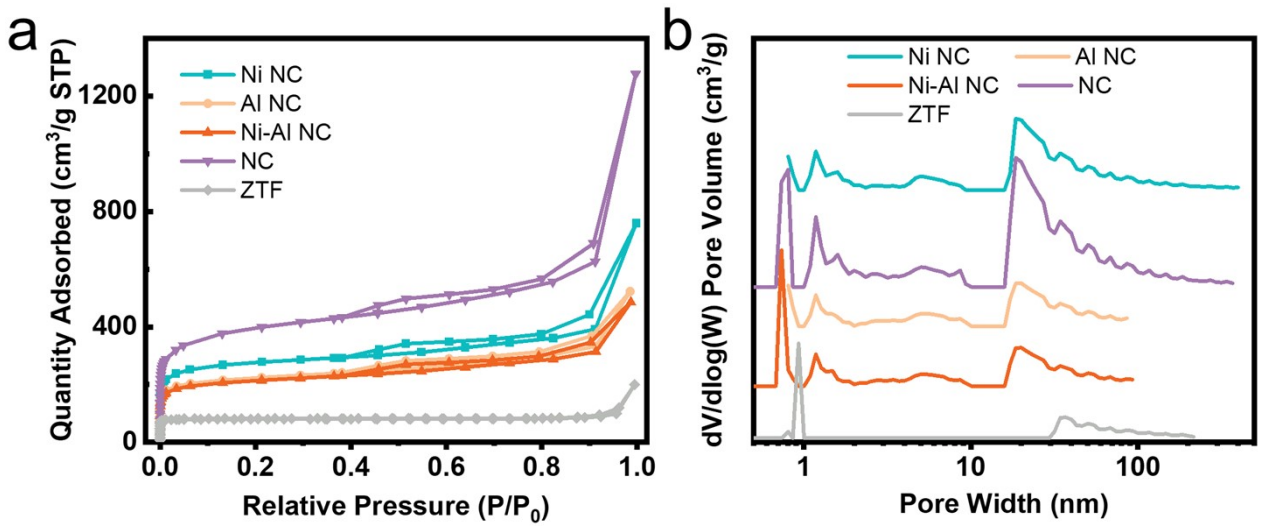

Figure S4. (a) N_2 adsorption-desorption isotherms of ZTF, NC, Ni NC, Al NC, and Ni-Al NC; (b) pore structures of ZTF, NC, Ni NC, Al NC, and Ni-Al NC.

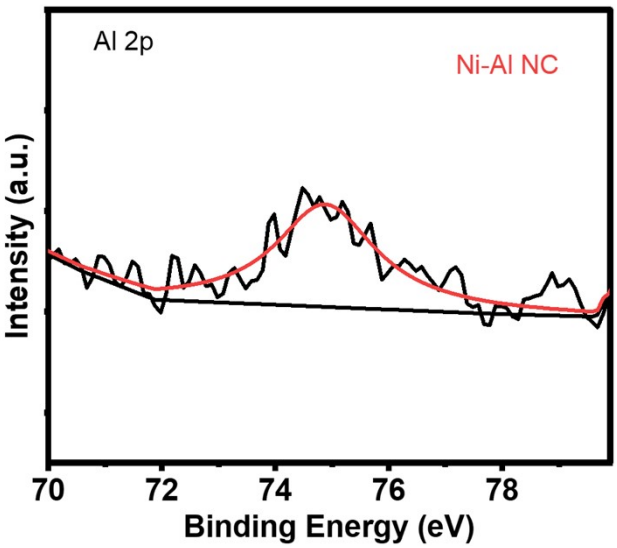

Figure S5. High-resolution XPS spectrum of the Al 2p of Ni-Al NC.

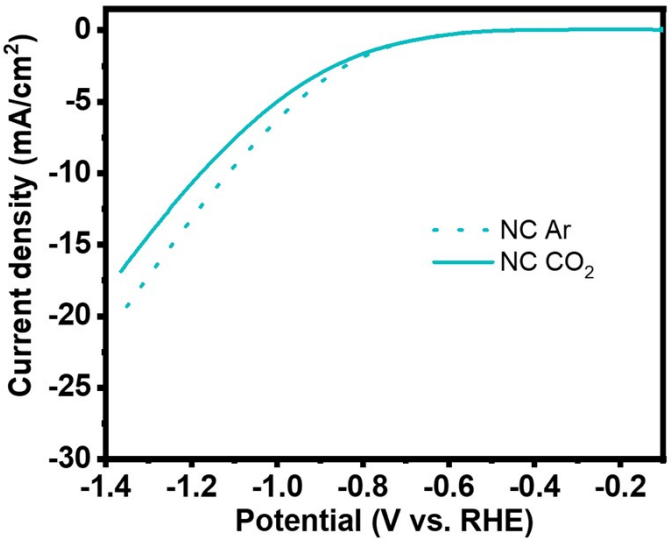

Figure S6. The LSV curves of support NC in the Ar-saturated (dotted line) and CO_2-saturated (solid line) 0.1 M $KHCO_3$ electrolyte.

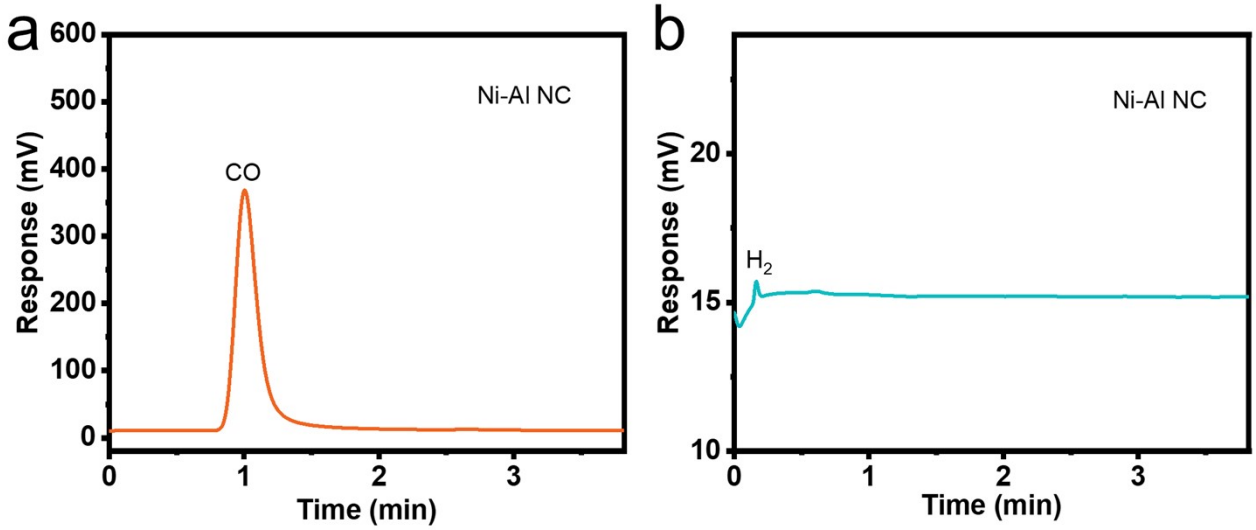

Figure S7. Representative spectra of (a) flame ionization detector (FID) and (b) thermal conductivity detector (TCD) taken for the Ni-Al NC at − 0.7 V vs. RHE.

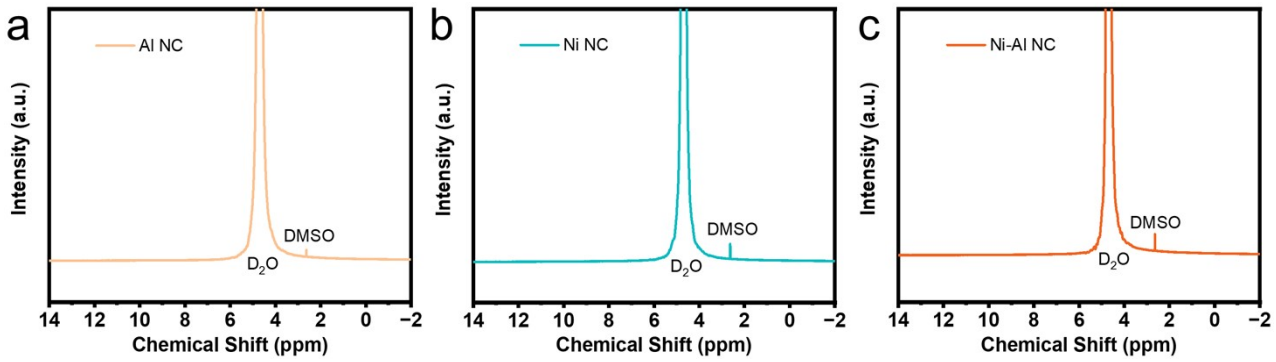

Figure S8. ^{1}H NMR spectra of the liquid product obtained over (a) Ni NC, (b) Al NC, and (c) Ni-Al NC after 1 h CO reduction at − 0.7 V vs. RHE.

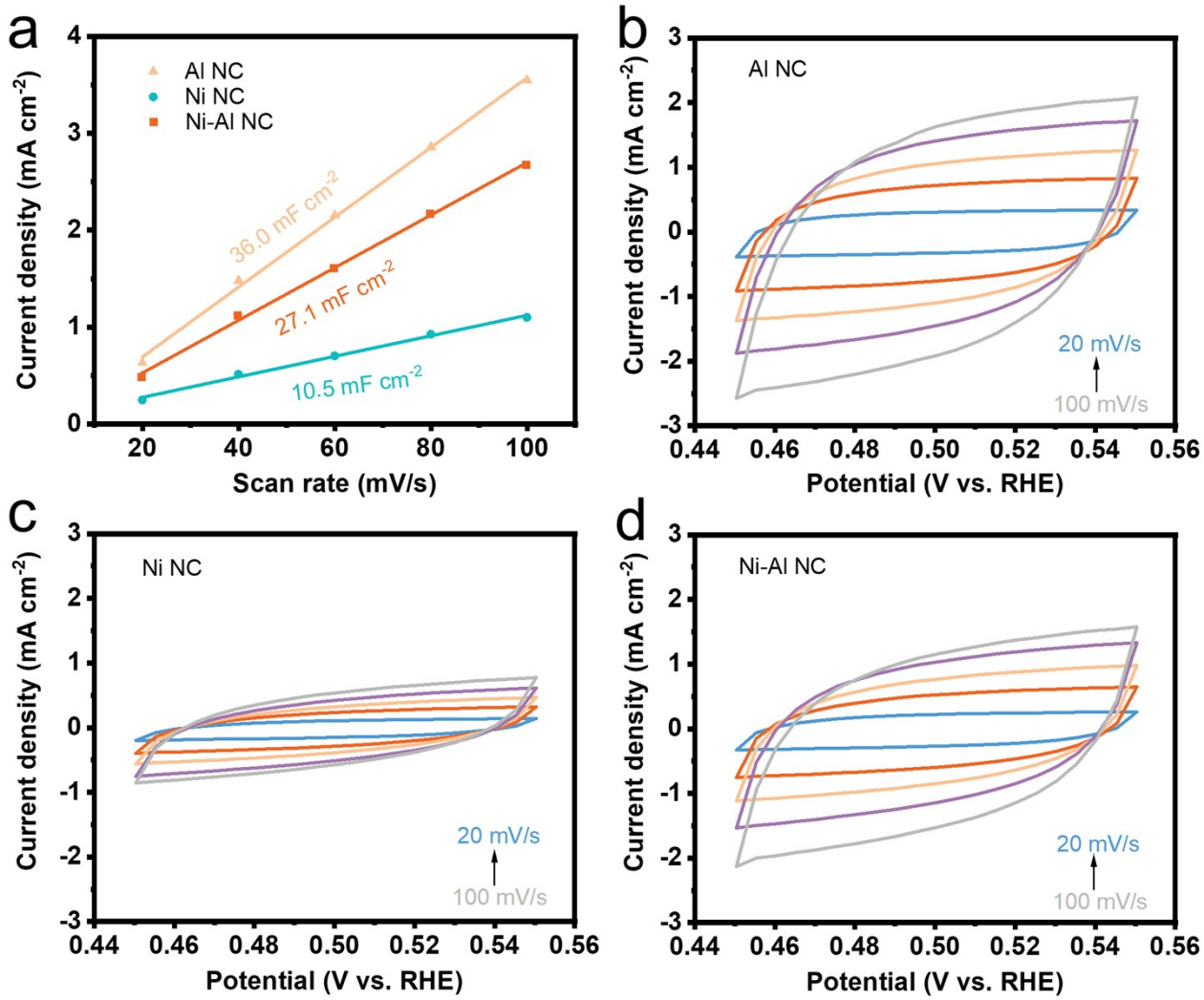

Figure S9. (a) Double layer capacitive currents plotted against scan rates performed in CO_2-saturated 1.0 M KOH solution. Cyclic voltammograms of (b) Al NC, (c) Ni NC, and (d) Ni-Al NC at different scan rates (20, 40, 60, 80, and 100 mV/s).

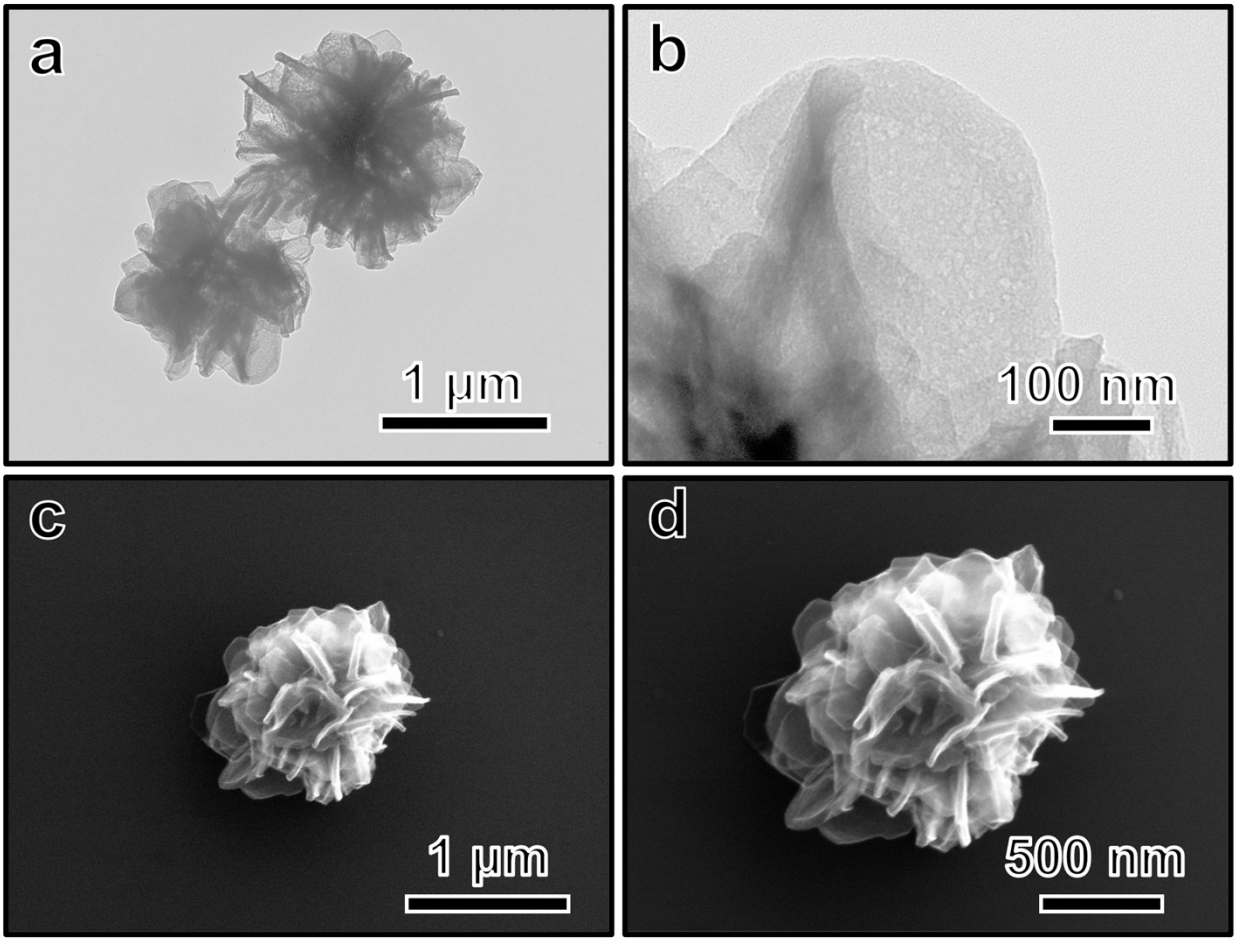

Figure S10. (a, b) TEM and (c, d) SEM images of the used Ni-Al NC.

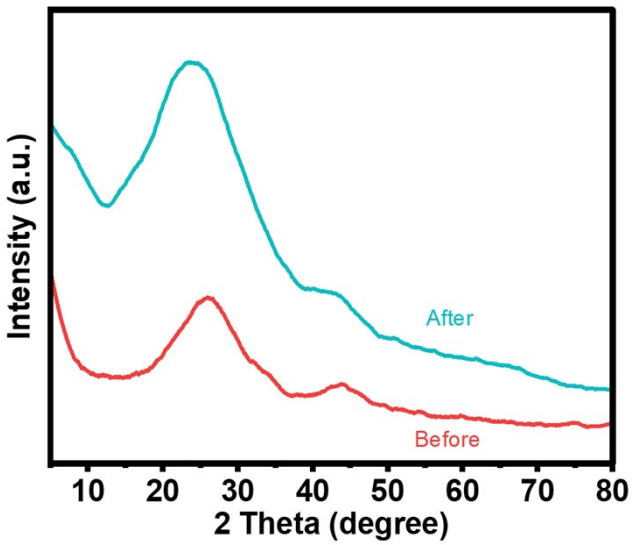

Figure S11. XRD patterns of Ni-Al NC catalyst before and after CO_2RR.

Table S1. BET analysis results of samples.

Catalysts	S_{BET} (m^2/g)[a]	V_{meso} (cm^3/g)[b]	V_{micro} (cm^3/g)[c]
ZTF	251.4	~	0.145
NC	1209.9	0.557	0.365
Al NC	697.7	0.552	0.236
Ni NC	877.3	0.353	0.311
Ni-Al NC	669.3	0.503	0.226

[a]: S_{BET} is BET specific surface area.

[b]: V_{meso} is the specific mesopore volume calculated from desorption isotherm by the BJH method.

[c]: V_{micro} is the specific micropore volume calculated by the *t*-plot method.

Table S2. Comparison between Ni-Al NC and other reported catalysts for CO_2RR.

Catalysts	Electrolyte	FE_{CO}/%	The potential of FE_{CO} above 90% (vs. RHE)	j_{CO} (mA cm^{-2})	The potential range of CO (mV)	Ref.
Ni-Al NC	**0.1 M $KHCO_3$**	**98**	**− 0.7 to − 1.0**	**14**	**300**	**This work**
Zn-N-G-800	0.5 M $KHCO_3$	90.8	− 0.5	4	~	[1]
$Zn_{94}Cu_6$	0.5 M $KHCO_3$	90	− 0.8 to − 0.95	9[a]	150	[2]
$[Au_{22}H_3]^{3+}$	0.5 M $KHCO_3$	92.7	− 0.6	5.4[a]	~	[3]
Ni NC@900	0.1 M $KHCO_3$	96	− 0.8 to − 1.0	16.2[b]	200	[4]
2-C16 Ag foil	~	97	− 0.8	~	~	[5]
NC@Ni/C-180	0.5 M $KHCO_3$	97	− 0.7 to − 1.1	4.5[a]	400	[6]
3D-h Cu-Sn	0.1 M $KHCO_3$	98.6	− 0.25 to − 0.6	0.5[a]	350	[7]
C-Bi_3Pd_{97}-SAA	0.5 M $KHCO_3$	91.5	− 0.4 to − 0.5	0.6[b]	100	[8]
Pd_2 DAC	0.5 M $KHCO_3$	98.2	− 0.7 to − 0.85	6.76	150	[9]
Ni-N/NPCNSs	0.1 M $KHCO_3$	90.7	− 0.74	3.8[b]	~	[10]
FeN_4Cl/NC-7.5	0.5 M $KHCO_3$	90.5	− 0.6	9.78	~	[11]
Ga-N_3S-PC	0.5 M $KHCO_3$	92	− 0.2 to − 0.3	18[a]	100	[12]
Cu-S_1N_3/Cu_x	0.1 M $KHCO_3$	100	− 0.55 to − 0.75	4[b]	200	[13]
Fe-N/P-C	0.5 M $KHCO_3$	98	− 0.4 to − 0.7	2[b]	300	[14]
O-Fe-N-C	0.5 M $NaHCO_3$	95	− 0.45 to − 0.5	4.2[b]	50	[15]
Ag-ZnO/$Ti_3C_2T_X$	0.5 M $KHCO_3$	98	− 0.87	22.59	~	[16]
V-$CuInSe_2$	0.5 M $KHCO_3$	91	− 0.7	8.5[b]	~	[17]

a This value is not mentioned in the article but is calculated from the current density and Faradaic efficiency.

b This value is not mentioned in the article but is derived from the graphical results.

References

1 Z. Chen, K. Mou, S. Yao and L. Liu, *ChemSusChem*, 2018, **11**, 2944-2952.

2 P. Moreno-García, N. Schlegel, A. Zanetti, A. Cedeño López, M. a. d. J. s. Gálvez-Vázquez, A. Dutta, M. Rahaman and P. Broekmann, *ACS Applied Materials & Interfaces*, 2018, **10**, 31355-31365.

3 Z.-H. Gao, K. Wei, T. Wu, J. Dong, D.-e. Jiang, S. Sun and L.-S. Wang, *Journal of the American Chemical Society*, 2022, **144**, 5258-5262.

4 R. Daiyan, X. Lu, X. Tan, X. Zhu, R. Chen, S. C. Smith and R. Amal, *ACS Applied Energy Materials*, 2019, **2**, 8002-8009.

5 A. K. Buckley, T. Cheng, M. H. Oh, G. M. Su, J. Garrison, S. W. Utan, C. Zhu, F. D. Toste, W. A. Goddard III and F. M. Toma, *ACS Catalysis*, 2021, **11**, 9034-9042.

6 Q. Lu, C. Chen, Q. Di, W. Liu, X. Sun, Y. Tuo, Y. Zhou, Y. Pan, X. Feng and L. Li, *ACS Catalysis*, 2022, **12**, 1364-1374.

7 C. J. Yoo, W. J. Dong, J. Y. Park, J. W. Lim, S. Kim, K. S. Choi, F. O. Odongo Ngome, S.-Y. Choi and J.-L. Lee, *ACS Applied Energy Materials*, 2020, **3**, 4466-4473.

8 H. Xie, Y. Wan, X. Wang, J. Liang, G. Lu, T. Wang, G. Chai, N. M. Adli, C. Priest and Y. Huang, *Applied Catalysis B: Environmental*, 2021, **289**, 119783-119791.

9 N. Zhang, X. Zhang, Y. Kang, C. Ye, R. Jin, H. Yan, R. Lin, J. Yang, Q. Xu and Y. Wang, *Angewandte Chemie International Edition*, 2021, **133**, 13500-13505.

10 J. Pei, T. Wang, R. Sui, X. Zhang, D. Zhou, F. Qin, X. Zhao, Q. Liu, W. Yan and J. Dong, *Energy & Environmental Science*, 2021, **14**, 3019-3028.

11 Z. Li, R. Wu, S. Xiao, Y. Yang, L. Lai, J. S. Chen and Y. Chen, *Chemical Engineering Journal*, 2022, **430**, 132882-132890.

12 Z. Zhang, J. Zhu, S. Chen, W. Sun and D. Wang, *Angewandte Chemie International Edition*, 2023, **62**, e202215136.

13 D. Chen, L. H. Zhang, J. Du, H. Wang, J. Guo, J. Zhan, F. Li and F. Yu, *Angewandte Chemie International Edition*, 2021, **133**, 24224-24229.

14 K. Li, S. Zhang, X. Zhang, S. Liu, H. Jiang, T. Jiang, C. Shen, Y. Yu and W. Chen, *Nano Letters*, 2022, **22**, 1557-1565.

15 T. Zhang, X. Han, H. Liu, M. Biset-Peiró, J. Li, X. Zhang, P. Tang, B. Yang, L. Zheng and J.

R. Morante, *Advanced Functional Materials*, 2022, **32**, 2111446-2111453.

16 Y. Hao, F. Hu, S. Zhu, Y. Sun, H. Wang, L. Wang, Y. Wang, J. Xue, Y.-F. Liao and M. Shao, *Angewandte Chemie International Edition*, 2023, e202304179.

17 J. Wang, X. Zheng, G. Wang, Y. Cao, W. Ding, J. Zhang, H. Wu, J. Ding, H. Hu and X. Han, *Advanced Materials*, 2022, **34**, 2106354-2106361.